3. Materials and Methods

This chapter provides a detailed description of all the materials and methods used and implemented to achieve our research objectives. It deals with various designs, different analytical methods, and experimental procedures adopted to attain the objectives set for the present research. Moreover, the experimental plan, techniques, calculation procedures, and statistical tools employed in the study are discussed in this chapter. The methodology is systematically divided into multiple sections to facilitate understanding.

The first objective is the development of a solar-air-heating system (SAH) designed specifically for the newly developed integrated solar greenhouse drying system (ISGHD) for drying agricultural produce, with supported PV modules to run the blower and exhaust.

The second objective is the experimental performance of ginger drying using the solar drying method and the existing method for drying characteristics and quality attributes, as well as standardizing the operational parameters of the ISGHD for ginger drying based on product quality. This step is crucial in ensuring the efficiency of the system, with a specific emphasis on enhancing the quality of dried ginger. Applying various drying models for the validation of experimental data, the findings from this standardization process are systematically compared with established mechanical drying methods, providing valuable insights into the comparative advantages of the ISGHD.

The third objective introduces the thermal performance of the solar air heating system and the developed drying system in terms of energy and exergy analysis. Using a sophisticated computational approach, CFD is utilized to simulate the thermal performance of ginger drying within the developed ISGHD system. This simulation improves system design and clarifies heat transfer mechanisms during drying.

Fourthly, the environmental and economic sustainability of ginger drying in the ISGHD system.

A pictorial view of the overall frame of the workflow of the complete methodology is given in (Fig. 3.1).

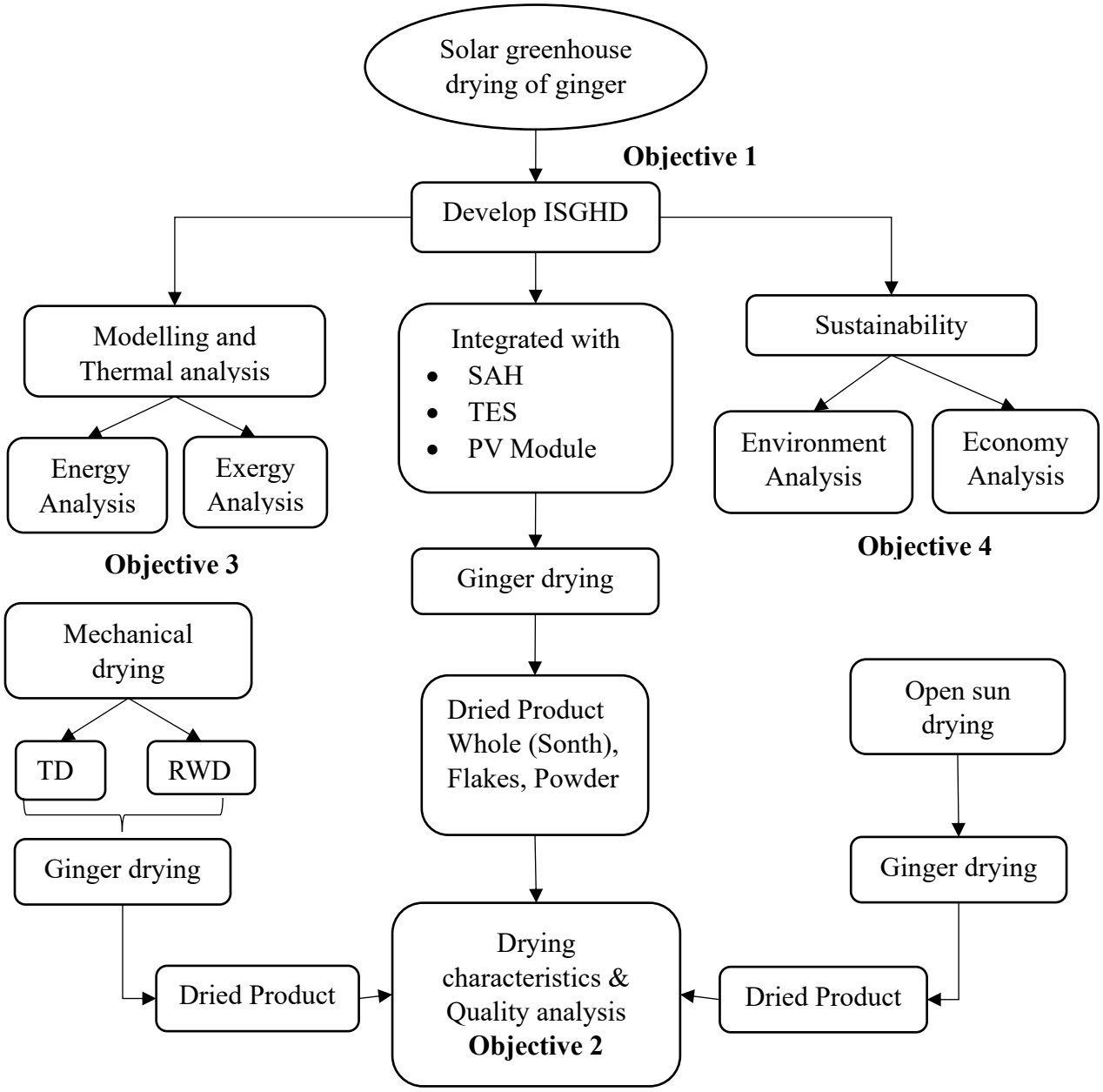

Fig. 3.1 Overall framework for the development of an integrated solar greenhouse drying system

3.1 Materials

3.1.1 Raw Material

Raw ginger, locally known as *Moran Ada* (*Zingiber officinale*), was obtained from the market in Tezpur, Assam, India, where a huge quantity of it is produced locally. As per the planned experiment, 10 kg of ginger was required for all drying methods, including solar drying and the

existing method. The ginger underwent cleaning, peeling, and slicing to achieve uniform thicknesses of (3.0-7.0) mm. Using the hot air oven method at 110°C for 24 hours, the initial moisture content of the ginger was determined to be 86% (w.b.). (Fig. 3.1.1) depicts images of both fresh ginger and slices of ginger.

Fig. 3.1.1 Fresh slices of ginger samples for the study

3.1.2 Instruments

The list of instruments, machines and components used, along with their model numbers, are detailed in Table 3.1.1. Instruments using for the experimental parameters, as given in (Fig. 3.1.2).

Table 3.1.1 Detail List of the major instruments used

Instrument	**Measurement/ Purpose**	**Model**	**Range**	**Reference Fig. 3.1.2**
Thermometer	Temperature	K type G-TECH GT 305-II	−200 °C to 1370 °C	(i)
Anemometer	Air flow	LCA301 (TSI Instrument, Malaysia	0-30 m/s	(ii)
Solarimeter	Solar radiation	Solar HT Kit Solarimeter PV204	-	(iii)
Speed controller	Blower and exhaust speed	Module 6V/24V/28V 3A 1203B		(iv)
Pyranometer	Solar radiation	SR11	0-2000 Wm^{-2}	(vi)
Data logger	Data store	Data Logger 4 Channels K-Type Thermometer	-200 to 1372°C	(vii)
Hot Air Oven	Moisture content	HAO1212	-	(viii)
Weighing balance	Weight	ME204, Mettler Toledo	0-1.0 kg	(ix)
Texture Analyzer	Texture	TA-HD Plus, UK	-	(x)
Colour meter	Colour	Ultra Scan VIS, Hunter Lab		(xi)

Fourier transform Infrared. Spectrophotometer	FTIR of ginger powder	Model: Frontier IR, Make: Perkin Elmer, USA	-	(xii)
Scanning electron microscope	Image	Model: JSM-6390LV Make: Jeol, Japan	-	(xiii)
X-ray Diffractometer	Ginger powder	D8 Focus Make: Bruker Axs Germany	-	(xiv)

(i)

(ii)

(iii)

(iv)

(v)

(vi)

(vii)

(viii)

(ix)

(x)

(xi)

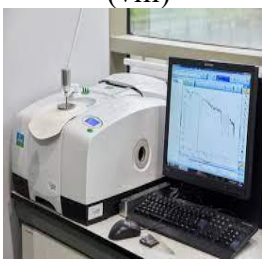

(xii)

(xiii)

(xiv)

Fig. 3.1.2 Instruments used for measurement in the experiment

3.1.3 Software

The lists of soft computing tools used for data handling, data extraction, curve fitting and statistical calculations are as follows

- IBM SPSS 25
- Origin Pro 8.5
- CATIA
- MATLAB R2018b
- COMSOL Multiphysics 5.2a

3.2 Methodology

3.2.1 Development of solar air heating system (SAH) and integrated solar greenhouse drying (ISGHD) system

Solar greenhouse drying for agricultural commodities provides farmers with a cost-effective and sustainable solution for post-harvest processing. By harnessing abundant solar energy, farmers can reduce operational costs associated with drying while improving product quality and extending shelf life. The controlled environment within the greenhouse protects crops from adverse weather conditions, ensuring consistent drying operations year-round. This versatility allows farmers to diversify their product offerings and adapt to changing market demands, ultimately empowering them to enhance their livelihoods and contribute to food security in their communities. Furthermore, solar greenhouse drying decreases the use of non-renewable energy, minimizing environmental impact and supporting a more sustainable agricultural system.

This section detailing the development of the SAH and ISGHD system is an advance of the solar greenhouse drying system (SGHD). Fig. 3.2.1 illustrates the development process of an integrated solar greenhouse drying system.

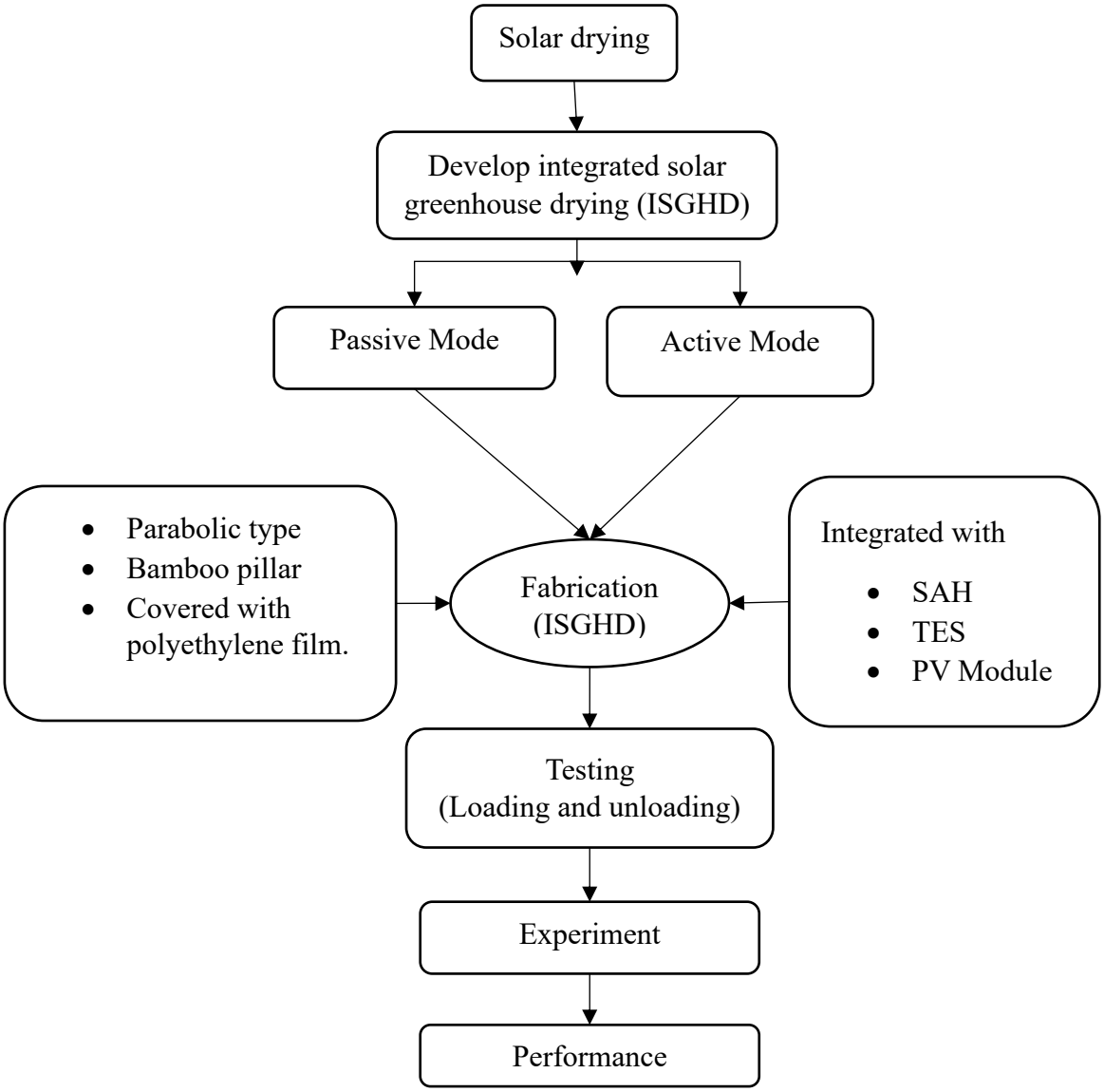

Fig. 3.2.1 Illustration showing the development process of an integrated solar greenhouse drying system

3.2.1.1 Solar air heating system (SAH)

Solar energy is the primary source for solar greenhouse dryers, fulfilling energy requisites for drying and storage during daylight periods through solar air heating. Prudent selection of the solar air heater assumes significance, taking into account parameters including solar irradiance, efficacy, and energy consumption. The dimensions of the heater are contingent upon solar irradiance, efficacy, and energy requisites, whereas efficiency depends on temperature, airflow rate, and heater surface area.

Assumptions for thermal analysis include

- Steady flow conditions
- Uniform wall temperature of the SAH
- Assumption of uniform fluid temperature
- Negligible side losses
- Duration of sunshine hour
- Total amount of heat required
- Average solar radiation

3.2.1.1.1 Flat-type solar air heater

A flat plate type solar air heating (SAH) system is integrated into a solar greenhouse dryer to supply hot air for the drying process. The SAH system consists of a flat plate area measuring (1.0L x 0.5 W) m^2, featuring an absorber plate crafted from a 1mm thick galvanized iron (GI) sheet coated in black for enhanced heat absorption. Furthermore, the absorber plate is reinforced by a 3mm thick galvanized iron sheet. Inside the SAH system, strategically positioned are five aluminium tubes with a diameter of 20 mm to convey hot air efficiently. One end of the system facilitates natural airflow, while the other end connects to a 30 mm diameter PVC outlet pipe for effective air distribution. This configuration ensures optimal airflow and heat transfer within the solar greenhouse dryer, thereby significantly improving the drying process. Fig. 3.2.2 shows the flat plate type solar air heater.

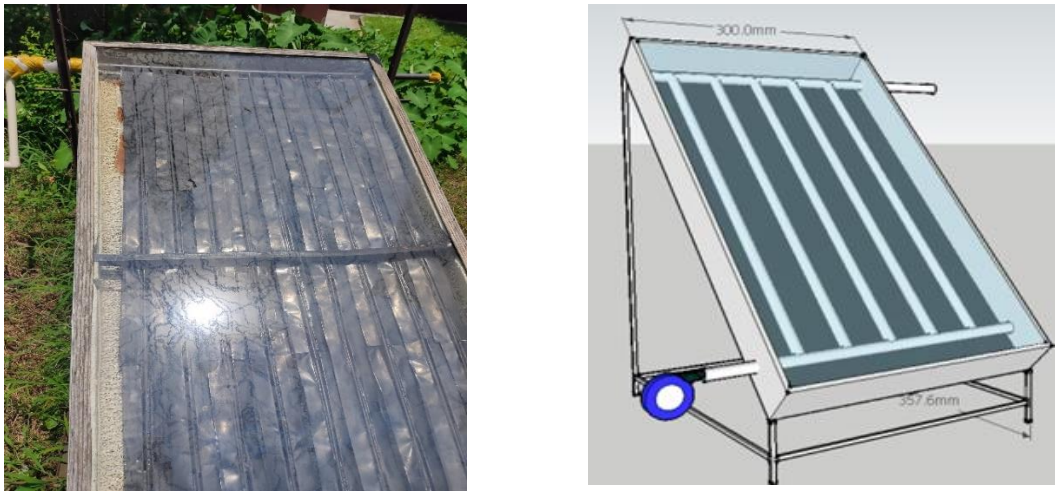

Fig. 3.2.2 Flat-type solar air heater

3.2.1.1.2 Corrugated type solar air heater (SAH with PCM)

To enhance the performance of the solar greenhouse dryer, a corrugated-type solar air heater (SAH) with PCM measuring (0.9 × 0.7 × 0.20) m was added. The collector was constructed using a 1 mm thick galvanized corrugated sheet painted black. A 3.0 mm thick glass layer was added to the absorber plate to trap solar radiation. The SAH collector was positioned facing south and tilted at 30 degrees. The SGHD system received the hot air that had been previously heated in the SAH through an insulated tube with a diameter of 50 mm, which was attached to one side of the dryer. Inside the SAH, paraffin wax, which is a PCM material, was filled. PCM material works as a latent heat storage system as well. PCM operates during periods without sunlight to regulate the internal dryer temperature, aided by PCM.

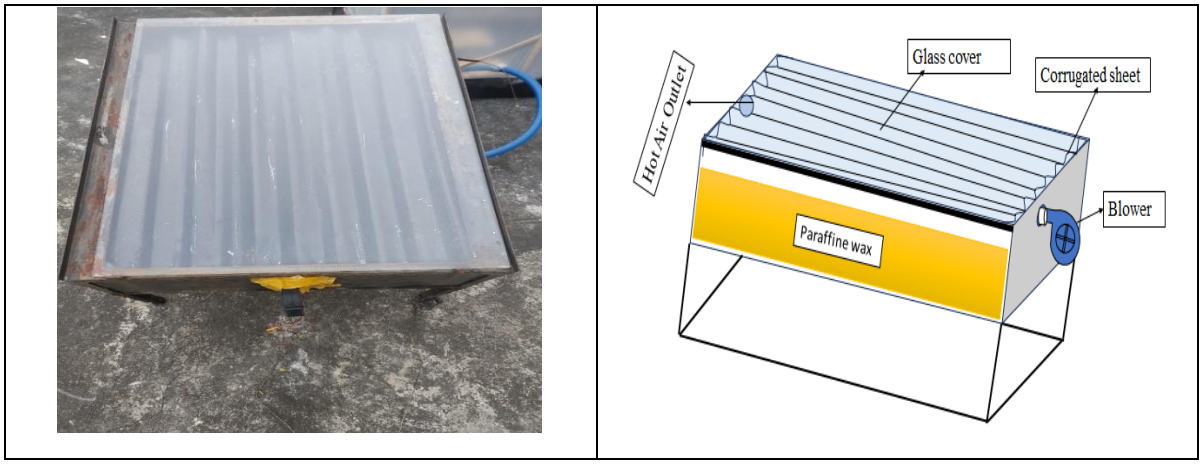

Fig. 3.2.3 Corrugated type solar air heater with PCM

Table 3.2.1 Dimension and properties of corrugated SAH with PCM

Component	Properties / Dimension
Area	(0.9L × 0.7W) m^2 and 0.2 m height
Absorber material	Galvanized corrugated sheet
Insulation	Expanded polystyrene foam and wool
Glazing	Window size Glass 3.0 mm
Absorptivity	0.95
Emissivity	0.92
Insulation Thermal conductivity	0.04 W/m·K
PCM (Paraffin wax)	Melting point 40-50 ^oC
Thermal conductivity of PCM	0.21 W/m·K

Fig. 3.2.3 shows the corrugated plate type solar air heater with PCM. All dimension and properties of corrugated plate type solar air heater are mentioned in Table 3.2.1

3.2.1.2 Development of integrated solar greenhouse drying system

The ISGHD system was created for drying, considering 4.0 kg of ginger per batch with an initial moisture content of 86% (w.b.) to a final moisture content of 10% (w.b.). The following assumptions and designs were considered to develop different components of the ISGHD system.

- Drying is presumed to take place under steady-state conditions.
- Thin-layer drying is adopted, with a maximum allowable drying bed thickness
- Uniform temperature distribution within the drying chamber is assumed.
- Determining the moisture removal requirements for the specified quantity of ginger.
- Selecting the total drying time based on daily sunshine hours.
- Calculating the necessary air quantity for the drying process.
- Solar radiation sunshine 8 hours.

3.2.1.2.1 Solar greenhouse drying, SGHD (Passive mode)

The Solar Greenhouse Drying (SGHD) is parabolic and even type, and the structural frame is covered with UV-stabilized polyethylene, which has a parabolic design made of bamboo. To reduce heat losses through ground contact, the bottom surface of the dryer is packed with black-painted rock and sand. Its floor size is (1.2 × 1.0) m², and its height from the ground at its centre is 1.0 m as shown in Fig. 3.2.4. The wire mesh drying tray has a surface area of (0.3 × 0.2) m², and it is also made black to absorb maximum solar radiation. The inclusion of a Photovoltaic (PV) Module, coupled with solar battery backup, ensures uninterrupted operation of the DC blower and exhaust fan. The fan plays an important role in removing moisture from the drying chamber. Fig. 3.2.5 shows an even span and parabolic type solar greenhouse drying.

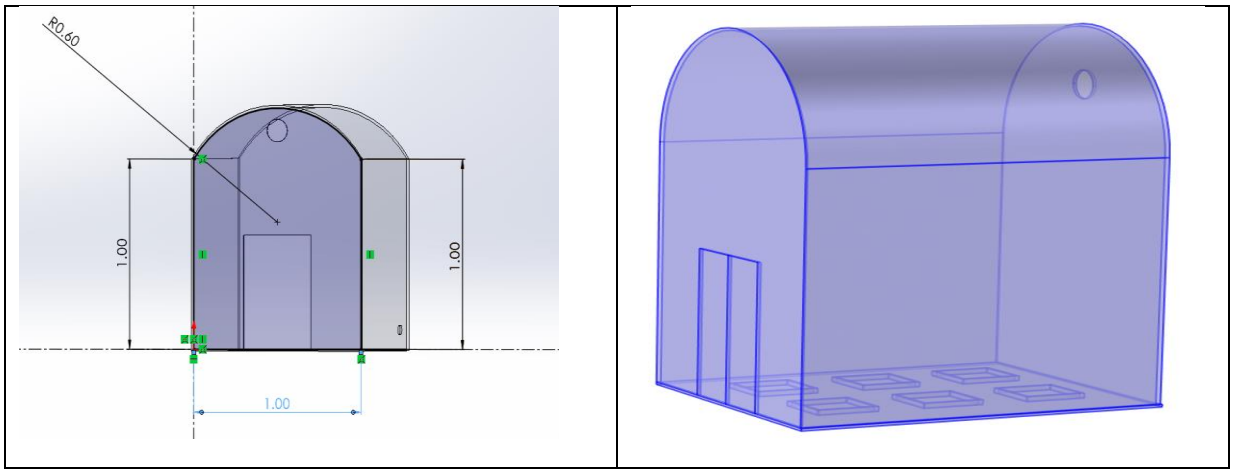

Fig. 3.2.4 3D Schematic diagram of solar greenhouse dryer

(a) (b)

Fig. 3.2.5 (a) even span SGHD and (b) parabolic SGHD

3.2.1.2.2 Integrated solar greenhouse drying, ISGHD (Active mode)

The integrated solar greenhouse drying (ISGHD) system with a solar air heater (SAH) and PV module has been developed at Tezpur University, Assam, India (26.63°N 92.8°E). This dryer represents an advancement of the SGHD passive mode dryer.

To improve the performance of the solar greenhouse drying system, we added a solar air heating system and PV module. Additionally, the integration of sensible heat storage (SHS) and phase

change material (PCM) extends the drying duration by retaining thermal energy storage when sunlight is not available. The inclusion of a Photovoltaic (PV) Module, coupled with solar battery backup, ensures uninterrupted operation of the DC blower and exhaust fan. The fan plays an important role in removing moisture from the dryer. Thus, integrated with the solar air heating system (SAH), photovoltaic (PV module), and thermal energy storage (TES), an integrated solar greenhouse drying (ISGHD) system is formed.

The developed ISGHD drying system with flat plate type SAH, as depicted in Fig. 3.2.6, and corrugated type SAH (with PCM), illustrated in Fig. 3.2.7, are presented. Table 3.2.2 outlines the components and specifications of the developed drying system. For the initial study, the investigation was conducted under the Flat plate type SAH. Subsequently, for better results, we developed the corrugated plate type SAH (with PCM) for enhanced efficiency.

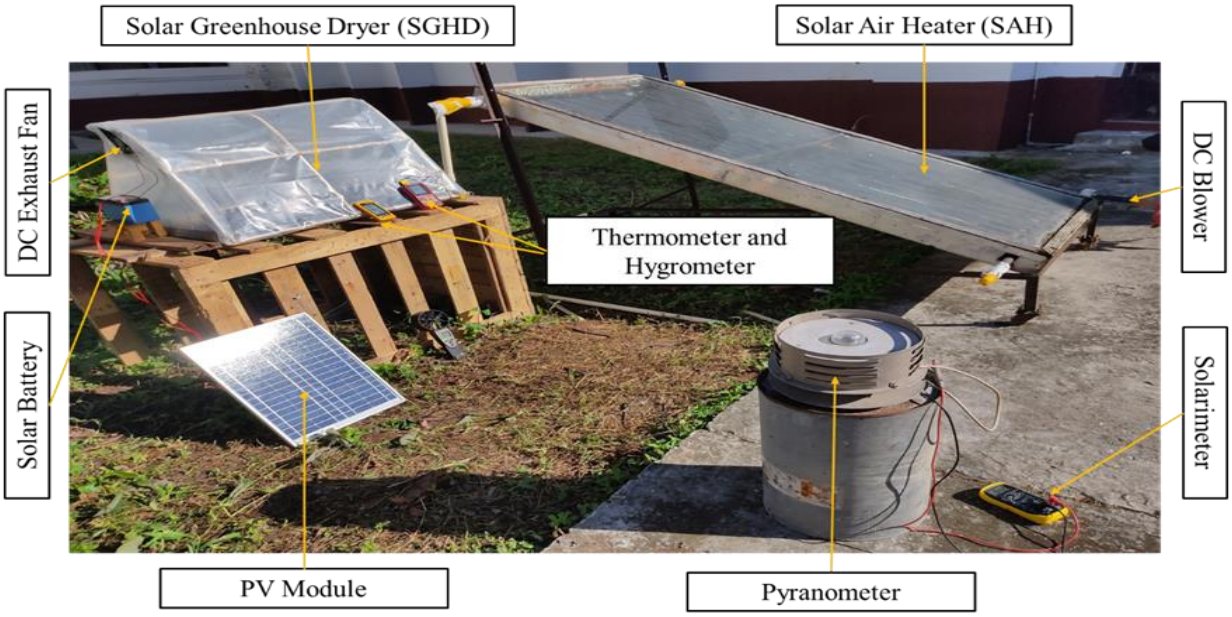

Fig. 3.2.6 Developed ISGHD system with flat plate type SAH

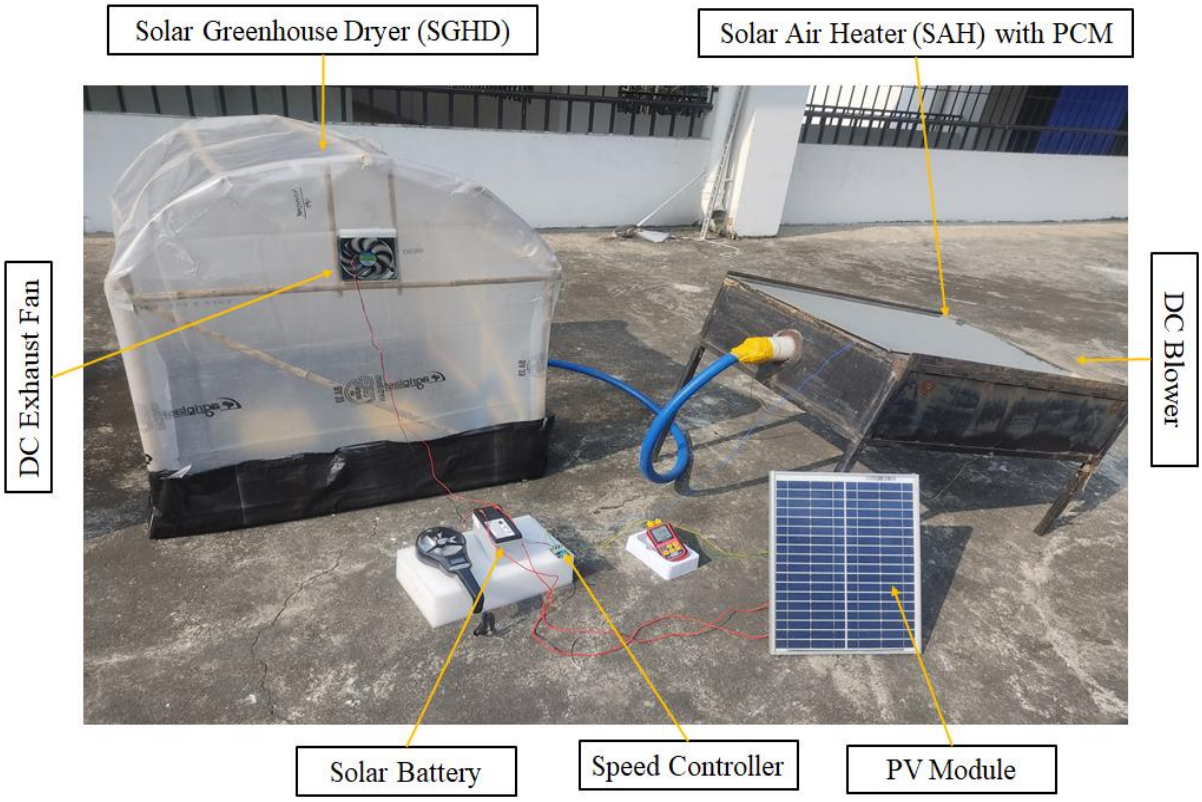

Fig. 3.2.7 Developed ISGHD system with corrugated type SAH

3.2.1.3 PV module panel

In the development of an integrated solar greenhouse drying (ISGHD) system using a photovoltaic (PV) module coupled with solar battery backup, ensuring uninterrupted operation of the DC blower and exhaust fan is crucial. The fan plays a pivotal role in removing moisture from the drying chamber. The PV module, rated at 50 W, and the DC solar storage battery, rated at 12V, work in tandem to power the system, as shown in Fig. 3.2.8. The PV module relies entirely on solar radiation to generate electricity for running the DC blower and exhaust fan. The blower is integrated into the solar air heating system and blows hot air at a predetermined mass flow rate controlled by a speed controller, as shown in Fig. 3.2.9. The PV module also powers the exhaust fan, and the solar battery provides backup power during off-sunshine hours and at night, ensuring continuous operation for about 4 to 5 hours. Overall, the PV module plays an important role in the creation of an integrated solar greenhouse drying system.

Table 3.2.2 Component and specification of developed integrated solar greenhouse drying system

S No.	Component		Specification/Capacity/Dimension
1	Solar greenhouse drying (SGHD)	a. Shape	Parabolic and Even span
		b. Area	(1.2L x 1.0W) m^2 and 1.0 m height
		c. Covered film	UV stabilized polyethylene
		d. Pillar	Bamboo
2	Corrugated type Solar air heater (SAH with PCM)	a. Type	Corrugated absorber plate type
		b. Area	(0.9L x 0.7 W) m^2
		c. Absorber plate	1.0 mm thick corrugated GI sheet black coated
		d. Galvanized iron sheet	3.0 mm
		e. PCM	Paraffin wax
		f. Glazing	Normal window glass 4mm thickness
		g. PVC pipe	30 mm diameter
3	Tray size	a. No. of tray	4.0 no.
		b. Size	(0.3Lx 0.2W) m^2
4	PV Module	a. Capacity	50 W, 12 V
5	Solar battery	a. Voltage	12V DC
		b. Storage	8.5 Ah
		c. Backup	4-6 h
6	Blower	a. Type	Axial
		b. Voltage	12V DC
		c. Speed	4000 rpm
		d. Air flow rate	1.064 m3/m
		e. Power	18 W
7	Exhaust fan	a. Type	Axial
		b. Voltage	12V DC
		c. Speed	2800 rpm
		d. Air flow rate	2.24 m^3/m
		e. Power	4.3W
8	Speed controller	a. Voltage	12-28V, DC motor
		b. Current	Within 3A

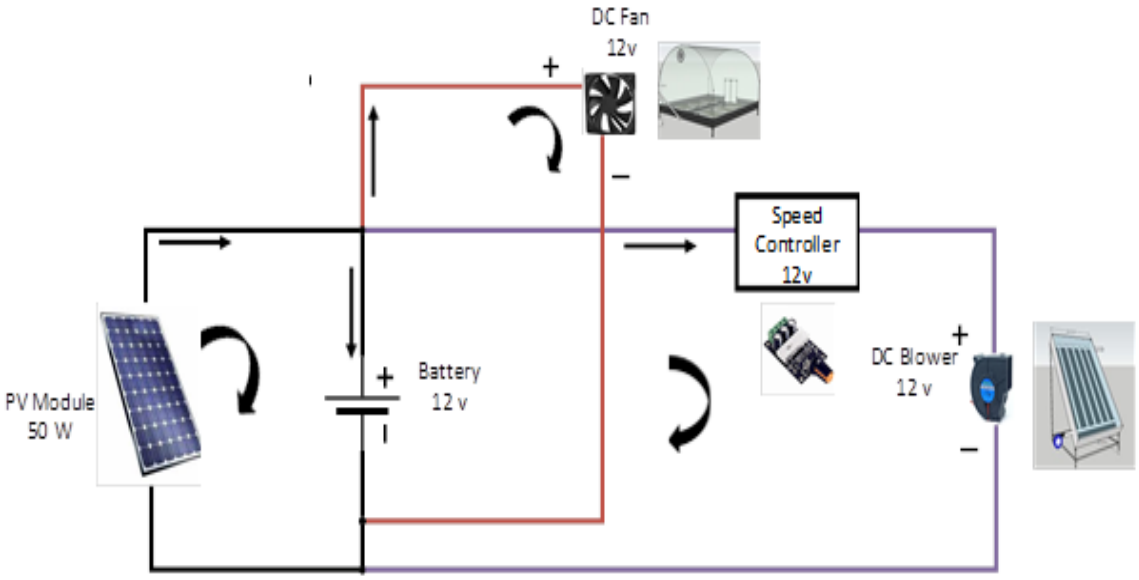

Fig. 3.2.8 The circuit diagram for the flow of DC current in the ISGHD drying system by PV module

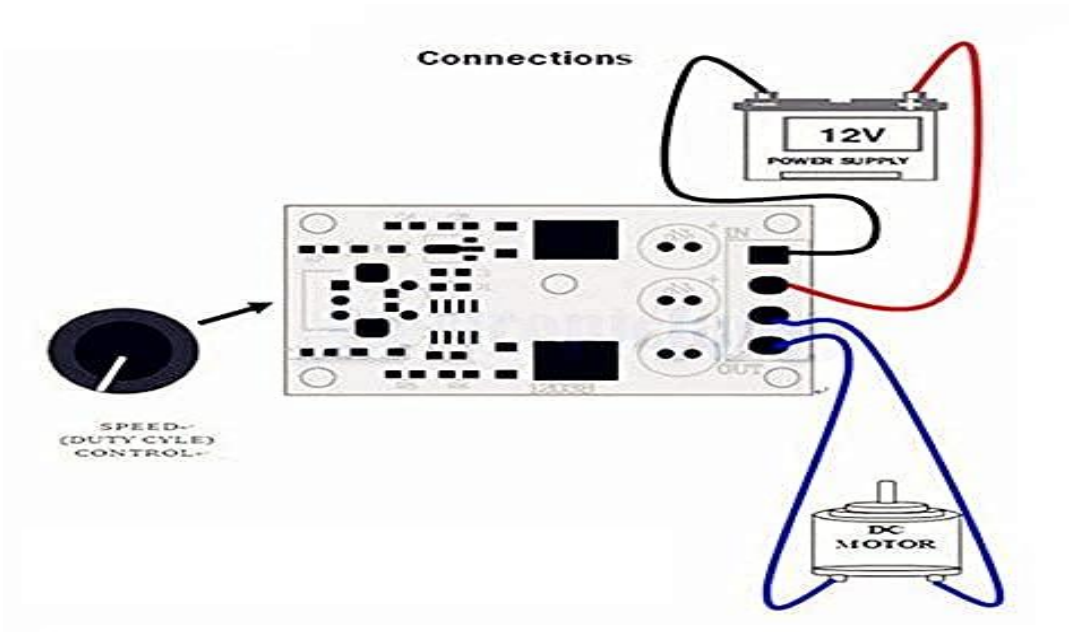

Fig. 3.2.9 Speed controller to control speed of exhaust and blower

3.2.1.4 Thermal energy storage (TES) system

The literature explores solar greenhouse dryers featuring integrated thermal energy storage, which typically utilize two main types: sensible and latent heat storage. Stone, pebble, brick, and

concrete, are common materials used in sensible heat storage systems. Paraffin wax, which has varying melting temperatures, is frequently used as the major latent heat storage medium in solar air heating systems. The storage material is integrated into the solar air heater, instantly harnessing solar radiation and combining thermal energy storage with air heating functions. TES material and their properties are present in (Table 3.2.3).

The variability of solar radiation presents a notable challenge for solar dryers, impacting their efficiency and product quality. Factors like limited sunlight, cloud cover, and fluctuations in solar radiation adversely affect drying performance and result in decreased product quality. Integrating thermal energy storage (TES) units addresses these challenges by enabling continuous drying during periods of sunlight scarcity, thereby preventing microbial growth and maintaining product quality. However, large TES units are required to sustain the drying process on cloudy days. TES materials store energy using sensible heat, latent heat, and thermochemical processes [14,17].

Table 3.2.3 TES material and their properties used in ISGHD for agriculture product drying

TES Material	Melting temperature (T_m)	Density (ρ) in kg/m^3	The heat of fusion (h_f) in kJ/kg	Specific heat (c_ρ) in kJ/kg K	Thermal conductivity k in W/m K	References
Rock	1800	2245-2566	100-400	710-920	2.7 - 3.0	[9,18,77]
Sand	1500	1400-1800	300-400	712	0.15- 0.30	
Paraffin wax	40-50	775-850	214	3.890	0.21	

3.2.1.4.1 Sensible heat storage (SHS) system

The study explores various heat storage options such as stone beds, water, concrete, and brick, with a specific emphasis on utilizing pebble stones to facilitate ginger drying, depicted in (Fig. 3.2.10). The quantity of stones required was determined based on the dryer's bed area, and their heat storage capacity was calculated considering density, specific heat, and thermal conductivity, all within the volume accommodated beneath the dryer bed area [9].

The sensible heat contained within a material can be calculated by Eq. (3.1)

$$Q = m_m C_p \ (T_f - T_i) \tag{3.1}$$

Here, Q represents the heat stored (J), m_m denotes the weight of material (kg), C_p is the specific heat of the material (J kg^{-1} K^{-1}), T_i stands for the initial temperature (°C), and T_f represents the final temperature (°C).

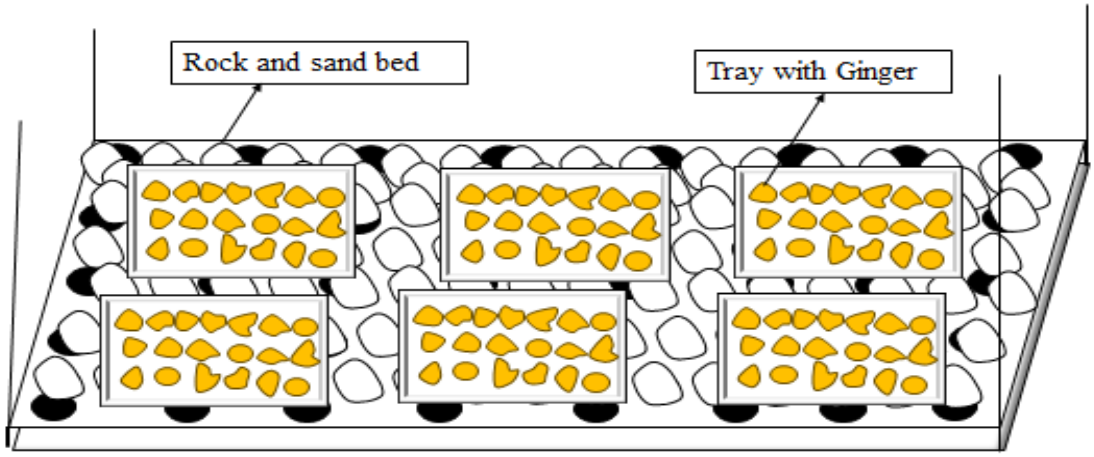

Fig. 3.2.10 SHS system inside the drying chamber

3.2.1.4.2 Latent heat storage (LHS) system

In the corrugated plate type solar air heater (SAH), phase change material (PCM) acts as a solar energy reservoir (Fig.3.2.11), typically utilizing paraffin wax to enhance drying rates under sunlight. PCM stores solar energy through phase change, enhancing drying efficiency. Equation (Eq. 3.2) quantifies the heat stored in Latent Heat Storage (LHS) materials like paraffin wax [14,17].

$$Q = m_m[C_{ps}\ (T_m - T_i) + L + C_{pl}\ (T_f - T_m)] \quad (3.2)$$

Here, Q represents the heat stored (J), m_m denotes the weight of material (kg), C_{ps} is the specific heat of the solid material (J kg^{-1} K^{-1}), T_i stands for the initial temperature (°C), C_{pl} represents the specific heat of the liquid material (J kg^{-1} K^{-1}), T_f denotes the final temperature (°C) and Tm is the melting point temperature (°C)

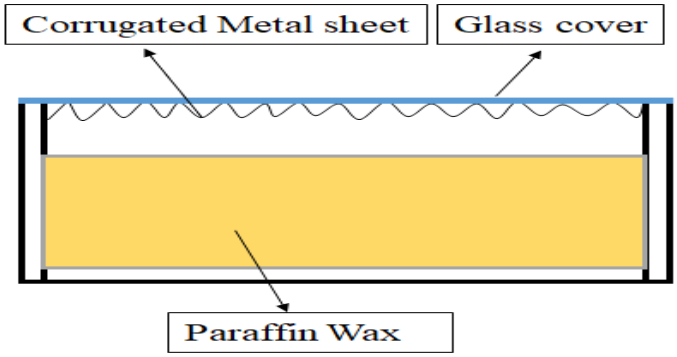

Fig. 3.2.11 PCM system inside the corrugated type SAH

3.2.2 Experimental performance of ISGHD system for ginger drying

The experiments conducted in developing the integrated solar greenhouse drying (ISGHD) aimed to optimize ginger drying. The objective was to assess the drying kinetics under varying environmental conditions, comparing various drying methods: open sun drying, OSD (Natural, conventional mode), solar greenhouse drying, SGHD (Passive mode), integrated solar greenhouse drying, ISGHD (Active mode) and existing mechanical drying such as refractance window drying (RWD) and tray drying (TD). Parameters such as moisture content (MC), moisture ratio (MR), and drying rate (DR) were analyzed to determine the most effective drying method. Various drying models were applied and validated for accuracy. Additionally, an artificial neural network, ANN was employed to predict the kinetics of ginger drying. Beyond kinetics, the study delved into the quality analysis of the dried ginger product, assessing rehydration ratio, shrinkage ratio, colour, texture, essential oil content, and antioxidant properties. Further characterization through SEM, XRD, and FTIR analyses was performed to understand the properties of the resulting ginger powder. Fig. 3.2.12 shows the flow chart of ginger drying by using different drying methods.

3.2.2.1 Sample preparation

Raw ginger was purchased from a market in Tezpur, Assam, India, and cleaned, peeled, and sliced to a uniform thickness using a slicer (3.0, 5.0, and 7.0) mm. The ginger's initial moisture content was found to be 86% (w.b.) utilizing the hot air oven method at 110°C for 24 hours. A 4.0 kg sample was divided into four trays, each containing 1.0 kg. These trays were then loaded into the SGHD drier. Throughout the drying process, the weight of the samples was monitored every 30 minutes. Because of the climate in the northeastern region, which has only 8 hours of sunshine per day, drying trials were conducted between 8:00 a.m. and 4:00 p.m.

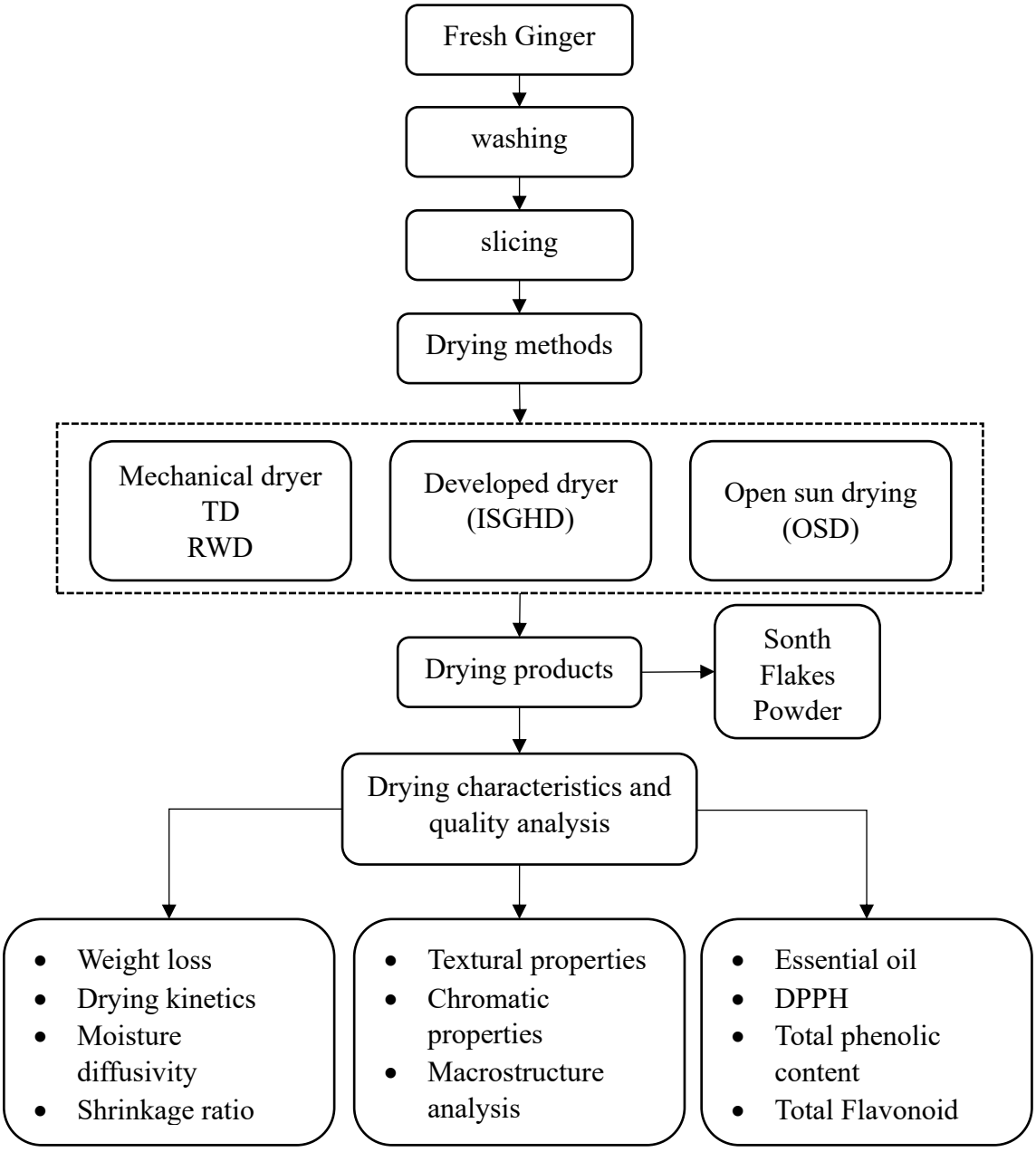

Fig. 3.2.12 Flow chart of ginger drying by using different drying methods

3.2.2.2 Drying method for drying

For the experiment using various drying methods: open sun drying, OSD (Natural, conventional mode), solar greenhouse drying, SGHD (Passive mode), integrated solar greenhouse drying, ISGHD (Active mode) and existing mechanical drying such as refractance window drying (RWD) and tray drying (TD), as shown in Fig. 3.2.13.

3.2.2.2.1 Open sun drying, OSD (Natural convectional mode)

Open sun drying was performed outdoors on an open ground surface, utilizing sunlight. Ginger slices were positioned on aluminium tray to dry. The samples' initial weights were recorded, and subsequent weight measurements were taken every hour until reaching the equilibrium moisture content. Every day from 8:00 a.m. to 4:00 p.m., the duration of drying time, relative humidity, and ambient temperature were recorded daily.

3.2.2.2.2 Solar greenhouse drying, SGHD (Passive mode)

Solar greenhouse drying will be performed under the developed solar greenhouse dryer, SGHD (Passive mode). The dryer's parabolic structural frame is covered with UV-stabilized polyethylene, which has a parabolic design made of bamboo. To reduce heat losses through ground contact, the bottom surface of the dryer is packed with black-painted rock and sand. Its floor size is (1.2 × 1.0) m^2, and its height from the ground at its center is 1.0 m. The wire mesh drying tray has a surface area of (0.3 × 0.2) m^2, and it is also made black to absorb maximum solar radiation. Inside the dryer, the black painted stone layer at the bottom for more thermal storage energy. Solar greenhouse drying is an eco-friendly and energy-saving technique to dry crops, herbs, fruits, and other items by harnessing solar energy. This process involves utilizing the sun's heat to create a controlled environment within a greenhouse, where the temperature and humidity can be regulated to facilitate the drying process. Detailed discussion given in (section 3.2.1.2.1).

3.2.2.2.3 Integrated solar greenhouse drying, ISGHD system (Active mode)

The integrated solar greenhouse drying system (ISGHD) advances in active mode over SGHD (Passive mode). ISGHD is assisted with photovoltaic (PV) modules and a solar air heater with phase change material (SAH with PCM), maximizing energy efficiency and sustainability. Detailed discussion in (section 3.2.1.2.2) and integrated solar greenhouse drying system with corrugated type (SAH with PCM).

3.2.2.2.4 Tray Drying (TD)

The drying procedure was conducted using a tray dryer (UOP 8-A, UK), which includes essential components such as a drying chamber, heater, electric blower, and temperature and airflow velocity controllers. The tunnel tray dryer's drying chamber was 0.3 m × 0.3 m × 0.4 m, as shown in (Fig. 3.2.13). To ensure uniformity in air temperature and velocity within the dryer, the entire apparatus

was operated for a minimum of one hour before commencing each experimental session. Throughout the experiment, the temperature was maintained at 60 °C.

3.2.2.2.5 Refractance Window Drying (RWD)

Refractance Window Drying (RWD) is a unique method of drying that utilizes radiant energy from infrared light to dry fruits, vegetables, and herbs. This procedure involves placing the material to be dried in a thin layer on a transparent polymer film, which floats on a water bath maintained at a controlled temperature, allowing infrared radiation to penetrate the product. The material is then exposed to radiant heat emitted by electrically heated refractance window. RWD stands out for its capacity to provide uniform drying, minimize processing time, and preserve product quality, making it especially suitable for heat-sensitive items, as shown in Fig. 3.2.13. The temperature of the water bath was fixed at 100 °C so that the transparent plastic surface where ginger will dry maintains a temperature of around 60 °C.

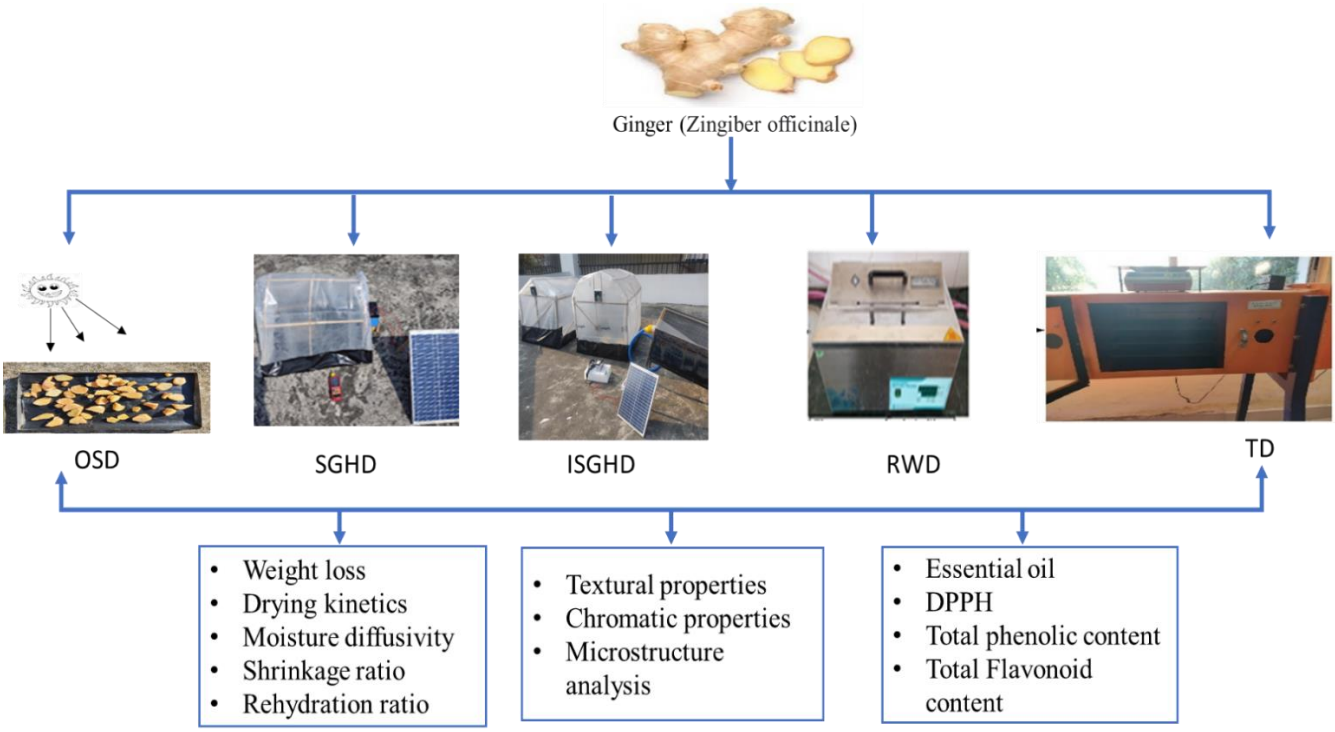

Fig. 3.2.13 Experimental methods for drying ginger and quality characteristics

3.2.2.3 Drying characteristics for ginger drying

The drying kinetics were analyzed for ginger slices in different drying methods: natural conventional (OSD), passive (SGHD), active (ISGHD), and existing (RWD and (TD). Parameters such as MC, MR, and DR were analyzed to determine the most effective drying method.

3.2.2.3.1 Moisture content (MC)

The moisture content of the dried ginger samples was assessed using the subsequent equations Eq. (3.3) & Eq. (3.4) [78,79].

$$MC\ (\%\ d.b.) = \frac{W_w}{W_d} \times 100 \tag{3.3}$$

$$MC\ (\%\ w.b.) = \frac{W_w}{W_w + W_d} \times 100 \tag{3.4}$$

Here, W_d represents the weight of dry matter (g), W_w is the weight of water (g), $MC\ (\%\ d.b.)$ stands for the moisture content on dry basis and $MC\ (\%\ w.b.)$ stands for the moisture content in wet basis

3.2.2.3.2 Moisture ratio (MR)

The moisture ratio (MR) is calculated by dividing the moisture content at any given time by the initial moisture content, both relative to the equilibrium moisture content, using the given (Eq. 3.5) [78,79].

$$MR = \frac{(M_t - M_e)}{(M_0 - M_e)} \tag{3.5}$$

Here, $M_t$stands for moisture content at each drying time, and M_0 and M_e refer to the initial and equilibrium moisture content of the material

3.2.2.3.3 Drying rate (DR)

Temperature, airflow, humidity, and the type of substance being dried all play significant roles in determining the drying rate. In general, an increase in temperature and airflow tends to enhance the drying rate by promoting faster evaporation of moisture calculated by Eq. (3.6.) [78,79].

$$Drying\ rate = \frac{M_t - M_{(t+dt)}}{dt} \tag{3.6}$$

Here, M_t represents the moisture content of the material at drying time t, $M_{(t+dt)}$ represents the moisture content of the material at drying time $(t + dt)$, and dt is the time interval over which the change in moisture content is measured

3.2.2.3.4 Moisture diffusivity

Moisture diffusivity indicates how efficiently moisture is removed. In the falling rate phase of food drying, moisture transfer prediction relies on mathematical models based on Fick's Law of diffusion. The effective moisture diffusivity was calculated utilizing the provided equations Eq. (3.7) & Eq. (3.8) [79].

$$\frac{\partial M}{\partial t} = \left(D_{eff} \frac{\delta^2 M}{\delta L^2} \right) \tag{3.7}$$

$$MR = \frac{M_t - M_e}{M_0 - M_e} = \frac{8}{\pi^2} exp\left(-\frac{\pi^2}{4} \frac{D_{eff} t}{L^2} \right) \tag{3.8}$$

D_{eff} is effective moisture diffusivity (m^2/s), t is drying time (s), and L is half of the thickness of the slab (m).

3.2.2.4 Drying kinetics model

Ten drying models were used to investigate the drying kinetics for ginger slices, and nonlinear regression analysis was performed using MATLAB R2018b and Origin Pro 2018 software. Drying kinetics models were customized according to MR values of ginger slices dried using different drying methods. Drying kinetics models are presented in Table 3.2.4.

Using (Eq. 3.9 - Eq. 3.11) for R^2, $\chi 2$ and RMSE were calculated accordingly.

$$R^2 = \frac{\sum_{i=1}^{n} \left(MR_i - MR_{pre,i} \right) \sum_{i=1}^{n} \left(MR_i - MR_{exp,i} \right)}{\sqrt{\left[\sum_{i=1}^{n} \left(MR_i - MR_{pre,i} \right)^2 \right] \left[\sum_{i=1}^{n} \left(MR_i - MR_{exp,i} \right)^2 \right]}} \tag{3.9}$$

$$\chi 2 = \frac{\sum_{i=1}^{n} \left(MR_{exp,i} - MR_{pre,i} \right)^2}{N - n} \tag{3.10}$$

$$RMSE = \left[\frac{1}{N} \sum_{i=1}^{n} \left(MR_{pre,i} - MR_{exp,i} \right)^2 \right] \tag{3.11}$$

Table 3.2.4 Outlines the drying models used for studying the drying kinetics of ginger slices

Model No.	Model Name	Equation	Reference
1	Newton	MR=exp(-kt)	[15,27,40]
2	Page	$MR=\exp(-kt^n)$	[15,40]
3	Modified Page	$MR=\exp(-kt)^n$	[52,80]
4	Henderson and Pabis	MR=a exp(-kt)	[27,40]
5	Logarithmic	MR=a exp(-kt)+c	[40]
6	Midilli and Kucuk	$MR=a\exp(-kt^n)+bt$	[52,81]
7	Wang and Singh	$MR = 1+ at + bt^2$	[27,40]
8	Diffusion approach	MR = a exp(-kt) +(1-a) exp(-kbt)	[15]
9	Two Term	$MR = a\exp(-k_1t)+ b\exp(-k_2t)$	[15,52,82]
10	Two Term exponential	MR = a exp (-kt) +(1 – a) exp(-kat)	[15,78]

3.2.2.4 Artificial neural network (ANN)

A feed-forward neural network design was implemented using the MATLAB R2018b programme to model ginger drying. 105 experimental data were used to execute ANN, and the data was split into three groups for training, testing, and validation, respectively: 70%, 15%, and 15%. As input data for the network, drying time (h), intensity solar radiation (Wm^{-2}), air temperature (^oC), MFR of air (kg/s), and relative humidity (%) values were used. As output data, MC, MR, and DR values were used [28,30].

3.2.2.5 Quality analysis of dried ginger

3.2.2.5.1 Rehydration ratio

The experiment involved rehydrating 3.0 g of dried ginger samples in a beaker filled with 100 mL of distilled water at room temperature. The rehydration process was monitored by taking samples at 30 minutes intervals until a stable weight was achieved. After rehydration, excess water was removed using filter paper, and the samples were weighed with an electronic balance (ME204, Mettler Toledo). Rehydration ratio calculated by using Eq. (3.12) [27,83].

$$R = \frac{W_r}{W_d} \tag{3.12}$$

Where, W_r Represent the drained weight of the rehydrated sample. and W_d Represent the Weight of the dried sample used for rehydration.

3.2.2.5.2 Shrinkage Ratio

The dried sample's shrinkage ratio was evaluated with the toluene displacement method. The proportion was computed by expressing the percentage change in volume from the initial apparent volume by Eq. (3.13) [84].

$$S = \frac{V_r}{V_o} \tag{3.13}$$

Where, V_r The volume displaced by the dried sample and V_o The volume displaced by fresh sample

3.2.2.5.3 Texture

The crushing strength of the dried ginger samples was evaluated using a texture analyzer (TA-XT, Surrey, UK). The maximum force (g) required to overcome the sample's compression resistance to a cylindrical probe with a diameter of 3.0 mm was evaluated [27,85].

3.2.2.5.4 Essential oil

The hydro distillation method was used to extract the ginger essential oil. In this process, 50 g of dried ginger powder was placed in distilled water in a 1000 mL round bottom flask filled with distilled water. The flask was then placed on a heating mental set to 85 °C and left to distil for 4-5 hours. The steam produced is then condensed with cold water, and as it condenses, the oil separates from the water [86].

3.2.2.5.5 Colour properties

The colour of the dried ginger samples from OSD, SGHD, and ISGHD was assessed using a colorimeter. L* (lightness: 0 = black, 100 = white), a* (red-purple: positive, bluish-green: negative), and b* (yellowness: positive, blueness: negative) were measured. The subscript '0' represents the values of the fresh ginger sample The colour variation (ΔE) among the dried ginger samples was computed by using (Eq. 3.14) [83,87].

$$\Delta E = \sqrt{(L^* - L_0^*)^2 + (a^* - a_0^*)^2 + (b^* - b_0^*)^2} \tag{3.14}$$

3.2.2.5.6 Total phenolic content (TPC)

The total phenolic content (TPC) in ginger was measured using the Folin Ciocalteu assay. For this, 400 µL of the samples were placed into test tubes, followed by 2.0 mL of Folin Ciocalteu phenol reagent (diluted tenfold with deionized water). After incubating for 5 minutes, 3.0 mL of a 7.5% (w/v) sodium carbonate solution was added. The absorbance was then read at 765 nm using a spectrophotometer after a 2-hour reaction in darkness. A blank was prepared by adding 400 µL of 80% methanol instead of the sample. The total phenolics were quantified as gallic acid equivalents (GAE), expressed in milligrams per gram of dry sample [58].

3.2.2.5.7 Total flavonoid content (TFC)

Total flavonoid content (TFC) in dried ginger extracts, 2.0 mL of the diluted extracts were added to a 10 mL volumetric flask. First, 0.3 mL of 5% $NaNO_2$ was added, followed by 0.3 mL of 10% $AlCl_3 \cdot 6H_2O$ after 6 minutes. After another 6 minutes, 2 mL of 4% NaOH was introduced. Then, 5.4 mL of water was added to the flask after 15 minutes and mixed well. The absorbance of the resulting mixture was measured at 510 nm. A blank was prepared by adding 400 µL of 80% methanol instead of the sample. The total flavonoid content was quantified as rutin equivalents, expressed in mg/g of dry weight [58].

3.2.2.5.8 DPPH (2,2-diphenyl-1-picrylhydrazyl)

This assay relies on assessing the antioxidant scavenging capacity against the stable radical DPPH. The determination of the extract's antioxidant activity involved analysing. Various dilutions of the extract (0.4 mL) were added to 3.5 mL of 0.14 mM DPPH solution in methanol and shaken vigorously. A graph was plotted showing the relationship between antioxidant activity (%) and the amount of extract (mg) [58].

3.2.2.5.9 X-ray diffraction (XRD)

The crystallinity and structural characteristics of proteins in ginger powders of varying sizes were assessed using an X-ray diffractometer. The powdered samples were dispersed onto a stub and positioned within the chamber of an analytical X-ray diffractometer, utilizing CuKα radiation with a wavelength of 1.54 Å. The investigation aimed to understand any alterations in the crystallographic structure of the dried ginger powder. Wide-angle X-ray diffractograms were generated, covering a diffraction angle range of 10 to 40º with a granularity of 0.05º [61,88].

3.2.2.5.10 Fourier transform infrared (FTIR)

FTIR was used to assess molecular changes during the ginger drying process. Dried ginger was converted into powder form for analysis. FTIR spectra were recorded in the wavenumber range of 4000 to 400 cm^{-1} with a resolution of 4 cm^{-1}. This analysis was conducted using an Infrared Spectrophotometer (Model: Frontier IR, Make Perkin Elmer, USA). The chosen instrument allowed for precise examination of molecular vibrations and absorbance in the ginger samples, enabling a comprehensive understanding of the alterations in molecular composition occurring throughout the drying process [61,88,89].

3.2.2.5.11 Scanning Electron Micrograph (SEM)

To examine the microstructure changes in ginger during different drying processes, a scanning electron microscope (JEOL, Model-JSM6390LV) was used. A portion of the dried ginger was carefully extracted from both the surface and inner parts, each measuring 5 × 5 × 5 mm^3. Prior to imaging, ginger particles were gold-coated and then introduced into the SEM. The morphological characterization of the ginger particles was assessed using an accelerating voltage of 20 KV [83,85,89].

3.2.3 Thermal performance of solar sir heater (SAH) and integrated solar greenhouse drying (ISGHD) for ginger drying

Energy and exergy analyses were conducted to assess corrugated type SAH and ISGHD system under varying mass flow rates and climate conditions. The goal is to enhance system efficiency by minimizing inefficiencies. A model for energy and exergy calculations was developed, and CFD analysis simulated temperature and airflow inside the dryer shown in Fig. 3.2.14. This study aims to identify optimization opportunities for a more energy-efficient and effective drying system. Efficiencies of ISGHD system and SAH were then calculated [70,90].

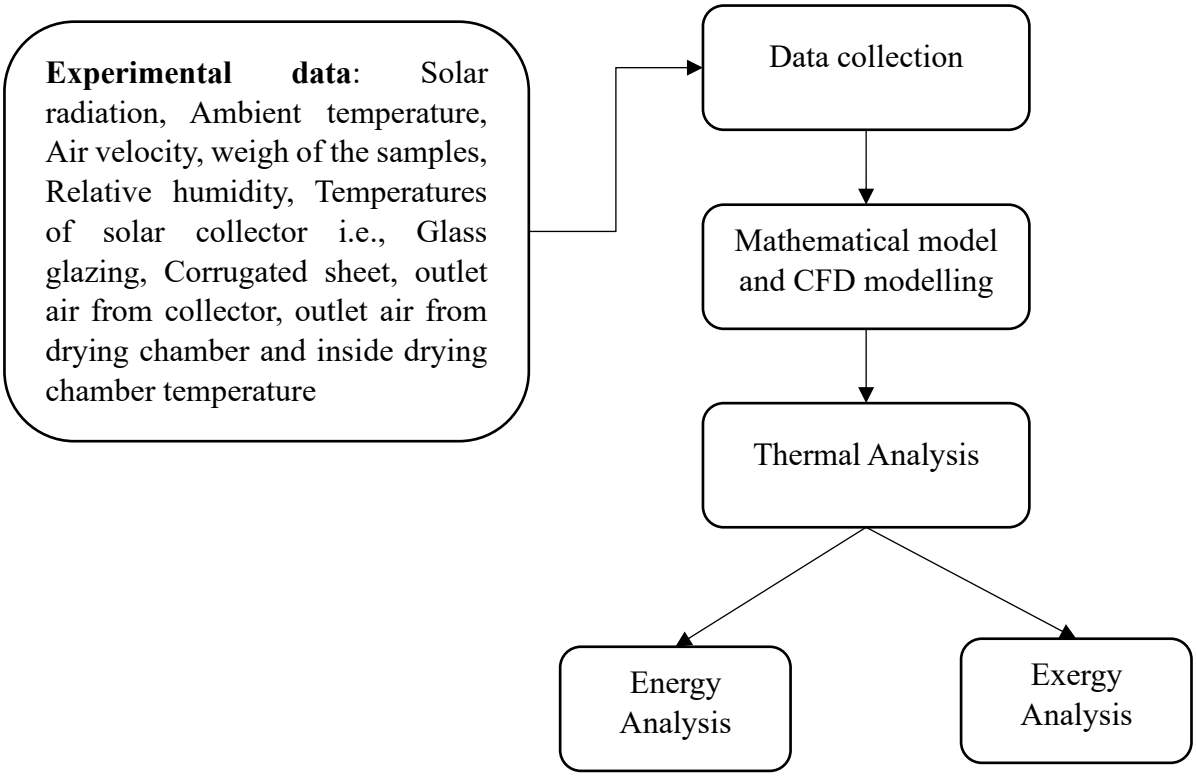

Fig. 3.2.14 Flow chart of energy and exergy analysis for the ISGHD

3.2.3.1 Energy analysis

Energy analysis is the method that is most frequently used to evaluate energy conversion systems. The fundamental law of thermodynamics serves as its foundation.

The calculation of energy analysis for the developed ISGHD system is given as given in (Eq. 3.15 – Eq. 3.22) [9,12,19,91,92].

The amount of useful energy gained is calculated as Eq. (3.15) & Eq. (3.16).

$$E_u = E_{out} = m_a\, c_a\, (T_o - T_i) \tag{3.15}$$

$$E_{in} = \alpha.\tau.I_{SAH}.A_{SAH} + E_{blower} \tag{3.16}$$

The thermal efficiency of SAH is given in Eq. (3.17 & Eq. (3.18)

$$\eta_{SAH} = \frac{E_{out}}{E_{in}} \tag{3.17}$$

$$\eta_{SAH} = \frac{m_a\, c_a\, (T_o - T_i)}{\alpha.\tau.I_{SAH}.A_{SAH}} \tag{3.18}$$

The specific energy consumption of a dryer is calculated by dividing the total energy used (kWh) by the weight of the water removed (kg) from the food product as in Eq. (3.19)

$$SEC = \frac{E_{total}}{m_w} \tag{3.19}$$

The drying chamber's overall energy consumption (E_{total}) is calculated as Eq. (3.20)

$$E_{total} = [(\alpha.\tau.I_{SAH}.A_{SAH}) + E_{blower} + (\alpha.\tau.I_{SGHD}.A_{SGHD})] \times t_{drying} \tag{3.20}$$

$$Q_{ev} = m_w \times \lambda \tag{3.21}$$

The overall dryer system's thermal efficiency calculated as Eq. (3.22)

$$\eta_{ISGHD} = \frac{Q_{ev}}{E_{total}} \tag{3.22}$$

3.2.3.2 Exergy analysis

Exergy of a system is the most beneficial work that may be done during a process, according to thermodynamics [12,13,19,32,91]. Calculated exergy efficiency as given Eq. (3.23) - Eq. (3.28).

$$Ex = m_a c_a \left[(T - T_{amb}) - T ln\left(\frac{T}{T_{amb}}\right)\right] \tag{3.23}$$

$$\sum Ex_{loss} = \sum Ex_{out} - \sum Ex_{in} \tag{3.24}$$

For exergy inlet

$$Ex_{in} = m_a c_a \left[(T_i - T_{amb}) - T_a ln\left(\frac{T_i}{T_{amb}}\right)\right] \tag{3.25}$$

For exergy outlet

$$Ex_{out} = m_a c_a \left[(T_o - T_{amb}) - T_a ln\left(\frac{T_o}{T_{amb}}\right)\right] \tag{3.26}$$

$$Exergy\ Loss = Exergy\ Inlet - Exergy\ Outlet \tag{3.27}$$

$$\eta_{ex} = \frac{Ex_{out}}{Ex_{in}} \tag{3.28}$$

3.2.3.3 Computational fluid dynamics (CFD) analysis and simulation

CFD-based analysis of ISGHD system and simulation of temperature and air flow rate distribution inside the chamber drying of the dryer by using COMSOL Multiphysics 5.2a software, as shown in Fig. 3.2.15 [69,70,93,94].

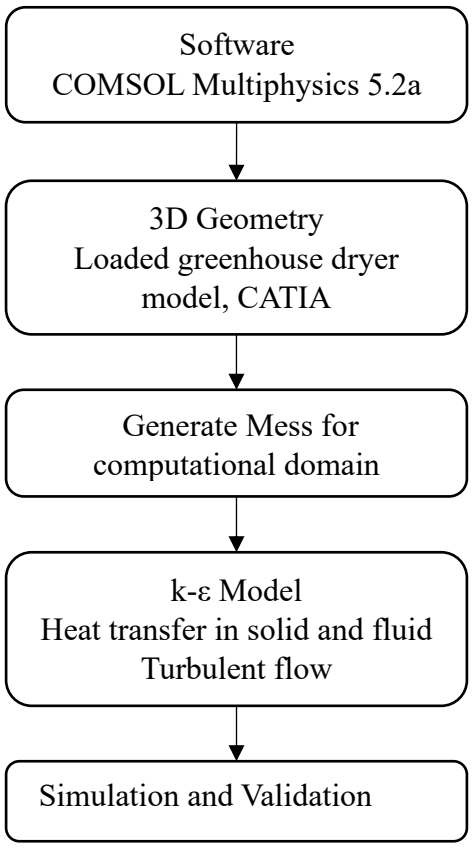

Fig. 3.2.15 Flow chart for simulation of the dryer using COMSOL Multiphysics

The computational framework used advanced software to solve the coupled Navier-Stokes and energy balance equations, employing the finite element (FE) method for a rectangular prism domain. Simulations focused on temperature, humidity, and airflow in the solar collector ducts and drying chamber, using the $k-\varepsilon$ turbulence model for accuracy. The thin fins' walls made internal conduction negligible, allowing detailed analysis of thermal and fluid dynamics, thus enhancing understanding of the system's performance evaluated, as given by (Eq. 3.29 - Eq. 3.31) [70,71].

Continuity equation as Eq. (3.29)

$$\frac{\partial \rho}{\partial t} + \nabla .\ (\rho\ \vec{v}) = 0 \tag{3.29}$$

Here, ρ is the fluid density, t is time, $\vec{v}$ is the velocity vector of the fluid, and $\nabla .$ denotes the divergence operator

Momentum equation Eq. (3.30)

$$\frac{\partial (\rho \vec{v})}{\partial x} + \nabla .\ (\rho\ \vec{v}\ \vec{v}) = -\nabla P + \nabla\ \bar{\tau} + \rho \vec{g} \tag{3.30}$$

Here, ρ is the fluid density, t is time, $\vec{v}$ is the velocity vector of the fluid, P is denoted the pressure, g is presented gravity

Energy equation Eq. (3.31)

$$\frac{\partial (\rho\ E_{total})}{\partial t} + \nabla .\ (\vec{v}(\rho E_{total}\ )) = \nabla .(-\vec{q} + \bar{\tau} .\vec{v}) \tag{3.31}$$

Here, ρ is the fluid density, t is time, $\vec{v}$ is the velocity vector of the fluid, q represents heat, E_{total} is the energy per unit mass

3.2.4 The environmental and economic sustainability of ISGHD system

This study aims to evaluate the environmental and economic feasibility (Fig. 3.2.16) of the integrated solar greenhouse drying (ISGHD) system developed for ginger drying. Environmental factors encompass energy payback time, embodied energy, CO_2 emissions, CO_2 mitigation, and the accrual of carbon credits. Economic evaluation will address initial investment, operational expenses, and total product drying costs.

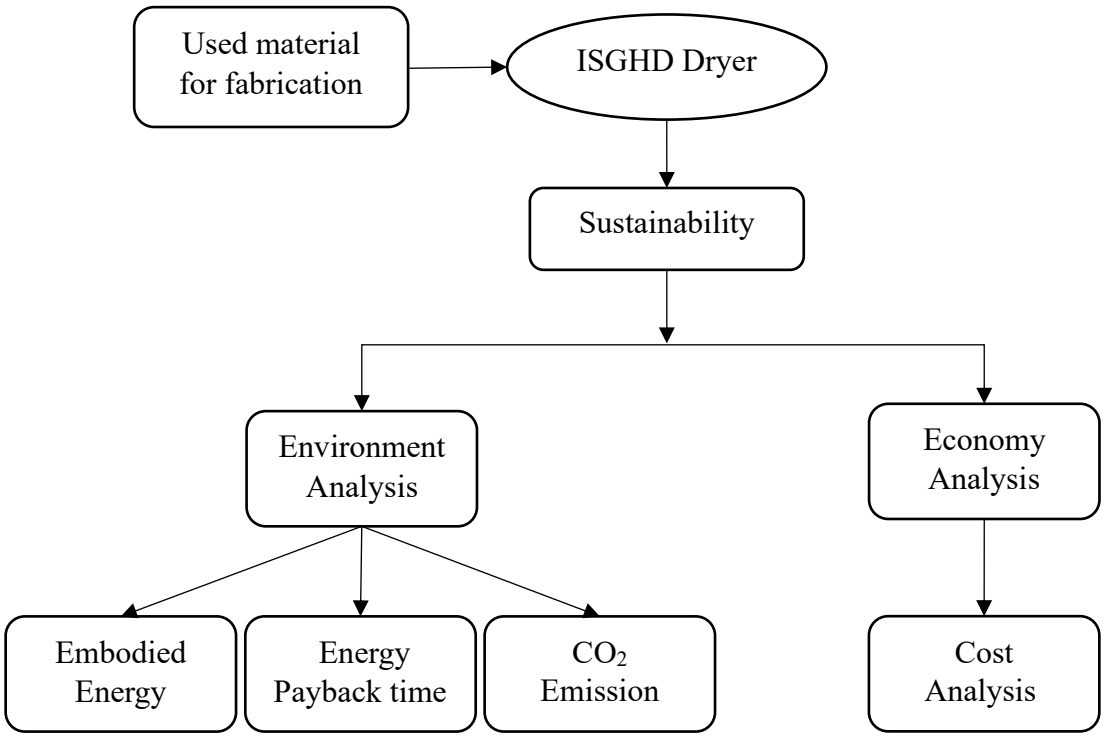

Fig. 3.2.16 Flow chart of Environmental and Economic evaluation for ISGHD system

3.2.4.1 Environmental analysis

3.2.4.1.1 Embodied energy

Embodied energy refers to the entire amount of energy consumed in the manufacturing and transportation of goods or services [37,95,96].

3.2.4.1.2 Energy payback time (EPBT)

EPBT is the duration required to recoup the total energy expended in preparing the materials, also known as embodied energy, for manufacturing the integrated solar greenhouse dryer [37,95–98]. Energy payback time is calculated using by Eq. (3.32).

$$Energy\ payback\ time\ (EPBT) = \frac{Embodied\ Energy\ (kWh)}{Annual\ Energy\ Output\ (kWh/year)} \quad (3.32)$$

3.2.4.1.3 Carbon dioxide emitted by the ISGHD system

The average CO_2 emissions from electricity generated by coal are equivalent to 0.98 kg of CO_2/kWh, as calculated by given Eq. (3.33) [37,96].

$$CO_2\ emmission\ per\ year = \frac{Embodied\ Energy\ \times 0.98}{lifetime} \quad (3.33)$$

3.2.4.1.4 CO_2 mitigation by ISGHD system

Assessing climate change potential involves considering CO_2 mitigation measures. Using solar thermal energy and PV systems to power the dryer reduces CO_2 emissions compared to traditional fuel-based air heating and electricity generation. Calculated CO_2 mitigation by Eq. (3.34).

$$CO_2\ mitigation\ \left(\frac{kWh}{year}\right) = \frac{1}{1-Lda} \times \frac{1}{1-Ldt} \times 0.98 \quad (3.34)$$

3.2.4.1.5 Carbon Credit earned by ISGHD system

The carbon mitigation over the 20-year lifetime of the solar greenhouse dryer is calculated as total CO_2 mitigation minus total CO_2 emission, as given Eq. (3.35). This equals the annual energy output multiplied by the dryer's lifespan, minus the embodied energy times 2.042.

$$\begin{aligned} &Net\ Carbon\ Mitigation \\ &\quad = Annual\ energy\ output\ energy \times life\ time \times 2.042 \\ &\quad - Embodied\ energy \end{aligned} \quad (3.35)$$

3.2.4.2 Economic analysis

The economic analysis encompasses the expenses incurred in constructing, operating, and maintaining the solar greenhouse dryer [4,22,35,43,96,99].

1. The ISGHD system lifespan is set at 10 years.
2. Processing capacity is 4 kg per batch per day.
3. It operates for 190 days annually.
4. Annual maintenance costs amount to 3% of the solar dryer's yearly expenses.

C_a has been calculated as given in (Eq. 3.36 – Eq. 3.39)

$$C_a = C_{ac} + C_m - S_v + C_{acf} \quad (3.36)$$

Whereas, C_{ac} represents the annual capital cost, C_m denotes maintenance cost, S_v signifies salvage value and C_{acf} stand for the annual operational cost of fan (Eq. 3.36)

$$C_{ac} = C_c \times F_{cp} \tag{3.37}$$

C_c is the capital cost and F_{cp} rate of interest on the capital cost (Eq. 3.37)

The salvage value S_v can be determined using the provided (Eq.3.38)

$$S_v = C_c \times (1 - i)^n \tag{3.38}$$

Maintenance cost is 3% of the annual capital cost of the dryer (Eq.3.39)

$$C_{acf} = N_f \times P_f \times P_e \tag{3.39}$$

N_f represent the number of hours the fan runs in a year, P_f is denoted the rated power consumption of fan and P_e represent the unit charge for electricity

3.2.5 Uncertainty interpretation

Uncertainty is an examination of the unpredictability and error in finding values. In the equation, ΔR represents the overall uncertainty (%) while R and x represent the uncertainty function and the dimensional coefficient, respectively. The uncertainty of the parameters during the ginger drying experiment is given in (Table 4.3.2). The total uncertainty values for the dependent parameters were determined by given (Eq. 3.40), (Eq. 3.41) & (Eq. 3.42).

$$\Delta R = \left[\left(\frac{\partial R}{\partial x_1}\Delta x_1\right)^2 + \left(\frac{\partial R}{\partial x_2}\Delta x_2\right)^2 + \left(\frac{\partial R}{\partial x_3}\Delta x_3\right)^2 + \cdots + \left(\frac{\partial R}{\partial x_n}\Delta x_n\right)^2\right]^{\frac{1}{2}} \tag{3.40}$$

$$\Delta\eta_{SAH} = \left[\left(\frac{\partial \eta_{SAH}}{\partial m_a}\Delta m_a\right)^2 + \left(\frac{\partial \eta_{SAH}}{\partial T_{iSAH}}\Delta T_{iSAH}\right)^2 + \left(\frac{\partial \eta_{SAH}}{\partial T_{oSAH}}\Delta T_{oSAH}\right)^2 + \left(\frac{\partial \eta_{SAH}}{\partial I_{SAH}}\Delta I_{SAH}\right)^2 + \left(\frac{\partial \eta_{SAH}}{\partial A_{SAH}}\Delta A_{SAH}\right)^2\right]^{\frac{1}{2}} \tag{3.41}$$

$$\Delta\eta_{ISGHD} = \left[\left(\frac{\partial \eta_{ISGHD}}{\partial T_{iISGHD}}\Delta T_{iISGHD}\right)^2 + \left(\frac{\partial \eta_{ISGHD}}{\partial T_{oISGHD}}\Delta T_{ISGHD}\right)^2 + \left(\frac{\partial \eta_{ISGHD}}{\partial I_{ISGHD}}\Delta I_{ISGHD}\right)^2 + \left(\frac{\partial \eta_{ISGHD}}{\partial T_{amb}}\Delta T_{amb}\right)^2 + \left(\frac{\partial \eta_{ISGHD}}{\partial A_{ISGHD}}\Delta A_{ISGHD}\right)^2\right]^{\frac{1}{2}} \tag{3.42}$$

3.2.6 Statistics analysis

Experimental analysis was conducted in triplicate, and mean values were derived from the resulting data. Ginger slice drying data, presented as moisture ratio (MR) versus drying time, were fitted to ten models. Goodness of fit was assessed using statistical parameters (R^2, $\chi 2$, and RMSE) calculated with Origin Pro 8.5 software. Additionally, analysis of variance and Turkey's test, performed using SPSS statistics 25 software, determined significant differences ($p \leq 0.05$) among variables of different drying methods and their effect on quality parameters.

3.3 Summary of chapter III

The first objective was the development of a solar air heating (SAH) system and an integrated solar greenhouse drying (ISGHD) system. Initially, a flat plate type solar air heating (flat type SAH) system was developed, followed by the development of a corrugated plate type (SAH with PCM) to enhance the efficiency of the drying system. The developed integrated solar greenhouse drying (ISGHD) system also includes provisions for a thermal storage system (TES) to enhance dryer effectiveness. The second objective is the experimental performance of ginger drying using different drying methods: Open sun drying, OSD (Natural, conventional mode), solar greenhouse drying, SGHD (Passive mode), integrated solar greenhouse drying, ISGHD (Active mode) and existing mechanical drying such as Refractance window Drying (RWD) and tray drying (TD). Drying characteristics, including moisture content (MC), moisture ratio (MR), and drying rate (DR), were examined to determine the most effective drying method. Various drying models were applied and validated for accuracy. Additionally, ANN was employed to simulate the kinetics of ginger drying. Beyond kinetics, the study delved into the quality analysis of the dried ginger product, assessing the rehydration ratio, shrinkage ratio, colour, texture, essential oil content, and antioxidant properties. Further characterization through SEM, XRD, and FTIR analyses was performed to understand the properties of the resulting ginger powder. Applying various drying models for the validation of experimental data, the findings from this standardization process are systematically compared with established mechanical drying methods, providing valuable insights into the comparative advantages of the ISGHD system. The third objective was the thermal performance of the solar air heating system and the developed dryer in terms of energy and exergy analysis. Using a sophisticated computational approach, computational fluid dynamics (CFD) was utilized to simulate the thermal performance of ginger drying within the developed ISGHD system. This simulation not only refines the system's design but also offers a detailed understanding of the convective and radiative heat transfer mechanisms at play during the drying process. The sustainability assessment of ginger drying in the ISGHD system addressed environmental and economic aspects. Environmental factors encompass energy payback time, embodied energy, CO_2 emissions, CO_2 mitigation, and carbon credit accumulation. The economic analysis examined initial investment, operational costs, and overall expenses related to product drying.